Clin Exp Metastasis (2013) 30:251–264
DOI 10.1007/s10585-012-9532-y

RESEARCH PAPER

S100P is a metastasis-associated gene that facilitates transendothelial migration of pancreatic cancer cells

Sayka Barry · Claude Chelala · Kate Lines · Makoto Sunamura · Amu Wang · Federica M. Marelli-Berg · Caroline Brennan · Nicholas R. Lemoine · Tatjana Crnogorac-Jurcevic

Received: 9 March 2012 / Accepted: 27 August 2012 / Published online: 25 September 2012

Abstract Pancreatic ductal adenocarcinoma (PDAC) is the 5th most common cause of cancer death in the UK and the 4th in the US. The vast majority of deaths following pancreatic cancer are due to metastatic spread, hence understanding the metastatic process is vital for identification of critically needed novel therapeutic targets. An enriched set of 33 genes differentially expressed in common between primary PDAC and liver metastases, when compared to normal tissues, was obtained through global gene expression profiling. This metastasis-associated gene set comprises transcripts from both cancer (S100P, S100A6, AGR2, etc.) and adjacent stroma (collagens type I, III, and V, etc.), thus reinforcing the concept of a continuous crosstalk between the two compartments in both primary tumours and their metastases. The expression of S100P, SFN, VCAN and collagens was further validated in additional primary PDACs and matched liver metastatic lesions, while the functional significance of one of the most highly expressed genes, S100P, was studied in more detail. We show that this protein increases the transendothelial migration of PDAC cancer cells in vitro, which was also confirmed in vivo experiments using a zebrafish embryo model. Thus S100P facilitates cancer cell intravasation/extravasation, critical steps in the hematogenous dissemination of pancreatic cancer cells.

Keywords Pancreatic adenocarcinoma · Liver metastasis · S100P · Transendothelial migration · Zebrafish

Sayka Barry and Claude Chelala equally contributed to this study.

Electronic supplementary material The online version of this article (doi:10.1007/s10585-012-9532-y) contains supplementary material, which is available to authorized users.

S. Barry · C. Chelala · K. Lines · N. R. Lemoine · T. Crnogorac-Jurcevic (✉)
Centre for Molecular Oncology, Barts Cancer Institute, Queen Mary University of London, Charterhouse Square, London EC1M 6BQ, UK
e-mail: t.c.jurcevic@qmul.ac.uk

M. Sunamura
First Department of Surgery, Tohoku University School of Medicine, Sendai, Japan

A. Wang
Immunology Department, Imperial College, London, UK

F. M. Marelli-Berg
Centre for Biochemical Pharmacology, William Harvey Heart Centre, Barts and the London SMD, Queen Mary University of London, London EC1M 6BQ, UK

C. Brennan
School of Biological Sciences, Queen Mary University of London, Mile End Road, London E1 4NS, UK

Introduction

Pancreatic ductal adenocarcinoma (PDAC) is one of the deadliest human malignancies. Despite substantial efforts, the incidence and mortality rate of this cancer remain unchanged with the 5-year survival rate being less than 5 % and the median survival time after diagnosis approximately 6 months [1]. One of the striking features of PDAC is its extremely aggressive nature with both local invasion and distant metastasis usually evident at presentation. The liver is the most common site of pancreatic cancer metastasis [2, 3] and secondary disease here is one of the major contributors to mortality of pancreatic cancer patients. Identifying the genes expressed in liver metastases and characterising signatures of haematogenous

progression could therefore be of particular importance since they would aid both in prediction of recurrence and serve as novel therapeutic targets for metastatic disease. However, research of this type has been hampered greatly in pancreatic cancer by the unavailability of metastatic specimens since resection is not undertaken in patients with known metastatic disease. Therefore, very few studies have reported the use of gene expression profiling to compare specimens of primary with metastatic lesions of pancreatic cancer, and very little is yet known about the underlying molecular mechanisms of liver metastasis in PDAC.

In their study, Niedergethmann et al. [4] reported differential expression in around 7 % of genes when they compared primary PDAC with tumour invasion front and liver metastases after implantation of MiaPaca2 cells in an orthotopic SCID mouse model. Campagna et al. [5] however, explored tissues derived from a rapid autopsy programme, where they compared the profiles of 19 primary and 11 matched (as well as 20 unmatched) metastases from different sites, including liver. They discovered no significant differences in gene expression patterns between primary and metastatic tissues, regardless of whether primary tumours were compared with matched or unmatched samples. These data resemble findings from similar profiling studies on other cancers where primary and metastatic lesions were compared [6–8].

A recent report on the timescale of PDAC progression indicated there is a substantial window of opportunity for the treatment of PDAC, which spans more than a decade for development of the primary tumour and at least an additional 3 years for metastases to develop [3]. Therefore the purpose of our study was to, by applying global gene expression analysis, uncover an enriched set of the most highly, commonly deregulated transcripts in both primary PDAC and liver metastatic lesions. Our hope in identifying such differentially expressed genes was that their gene products would, potentially, represent clinically relevant novel therapeutic targets.

Furthermore, the involvement of one such gene in the metastatic process, S100P, was studied in more detail.

S100P is a 10.4 kDa calcium binding protein that was previously shown to regulate growth and survival of pancreatic cancer cells, as well as increase their migratory and invasive capabilities. Moreover, decreased metastatic potential was noticed after silencing of S100P in the orthotopic mouse model [9]. In our previous study, we have shown that over-expression of S100P in Panc1 cells increases expression of cathepsin D, which facilitates local invasion by extracellular matrix (ECM) remodelling [10]; here, we demonstrate that S100P regulates intravasation/extravasation of pancreatic carcinoma cells both in vitro and in vivo, using zebrafish embryo model.

Materials and methods

Tissues and cell lines

Seven freshly frozen PDACs, 12 metastatic liver and three normal pancreas samples were obtained from Dr. Makoto Sunamura (Tohoku University, Japan) and from the Human Biomaterials Resource Centre, (Hammersmith Hospitals NHS Trust, London). All PDAC samples comprised 50–80 % of cancer cells, while liver metastatic specimens contained around 80 % of cancer cells. The utilised samples displayed predominantly moderate to poor differentiation.

Total RNA from normal liver was purchased from Ambion (at Invitrogen Life Technologies, Paisley, UK). Ten formalin-fixed, paraffin-embedded tissue samples of primary tumour and nine matched liver, and one lung, metastases were obtained from the Gastrointestinal Cancer Rapid Medical Donation Program (GICRMDP) developed at John Hopkins University, Baltimore, USA [11]. All specimens were obtained with full ethical approval from the host institutions.

The pancreatic cancer cell lines (Panc1 and BxPC3) were obtained from Cancer Research UK Cell Services, and cultured in DMEM high glucose, supplemented with 10 % heat-inactivated foetal calf serum (FCS; Gibco, Invitrogen Life Technologies) and 1:100 Pen/Strep. Establishment and characterisation of control (V3) and S100P-overexpressing stable cell lines (S5) has been described previously [10]. Primary cultures of human umbilical vein endothelial cells (HUVEC) were grown in RPMI medium supplemented with 20 % FCS, 12 Unit/ml heparin, 250 μg/ml Fungizone and 150 μg endothelial cell growth supplements. The identity of all the cell lines was verified by STR profiling.

RNA isolation and Affymetrix gene expression analysis

Total RNA was isolated from tissues with TRIzol Reagent (Invitrogen Life Technologies) and from cell lines using the RNAqueous RNA extraction kit (Ambion at Invitrogen Life Technologies), according to the manufacturer's protocol. Affymetrix human GeneChip HG-U133 set arrays (Affymetrix, Santa Clara, CA, USA) were used for gene expression analysis of tissue samples. Ten micrograms of total RNA was used for transcribing, labelling and hybridization to the arrays, all according to the manufacturer's instructions.

After scanning, raw.CEL files were analyzed using Bioconductor (http://www.bioconductor.org/) packages within the open source R statistical environment (www.r-project.org). The quality control metrics recommended by Affymetrix, the probe level models, box plots and intensity

histograms were used for quality assessment. After background correction by robust multi-array analysis, normalization by the quantiles method and summarization by the median polishing, a filter using the standard deviation of gene expression values to select the most variable 12,000 probes, was applied. For differential expression analysis, LIMMA [12] was used to fit a linear model to the normalized expression data for each probe followed by empirical Bayes smoothing. To account for technical replicates, the "duplicateCorrelation" function was used [13]. In order to obtain the intersection (enriched set of commonly deregulated genes between the primary PDAC and liver metastases), gene expression profiles were examined using a 2 × 2 ANOVA where two factors, status (tumour or normal) and organ (pancreas or liver) were contrasted. A double cut-off of false discovery rate <0.05 and a fold change ≥ 2 was used.

Quantitative reverse transcriptase PCR (QRT–PCR)

The gene-specific primer/probe set for S100P/Hs00195584_m1 (Gene symbol/TaqMan assay identity) was purchased from Applied Biosystems (Foster City, CA, USA). 1 μg of total RNA from individual tissue samples was reverse transcribed into complementary DNA (cDNA) using random hexamers and the Multiscribe reverse transcription kit (Applied Biosystems,) following the manufacturer's protocol. Real-time PCR reactions were prepared using Taqman Universal PCR Master mix (Applied Biosystems). Data was analysed according to the Standard Curve Method for relative quantification (Applied Biosystems). Standard curves were prepared for both the target (S100P) and the endogenous reference (18S). For each sample, the relative quantity of target and endogenous reference levels was determined from the appropriate standard curve. The target amount was then divided by the endogenous reference amount to obtain a normalised target value. The normal pancreas as well as normal liver were used as calibrators and each of the normalised target values was compared to the value of calibrators (arbitrarily set at 1) to generate the relative expression levels.

siRNA knockdown of S100P

Briefly, 2×10^5 S5 (S100P-overexpressing Panc1 cells) cells were plated in a 6-well plate. After overnight incubation, cells were transfected for 48 h with 40 nM ON-TARGETplus SMARTpool S100P siRNA or siCONTROL Non-Targeting siRNA pool 2 (Dharmacon, Thermo Scientific) using DharmaFECT siRNA Transfection Reagent 1 according to the manufacturer's instructions. Similarly, BxPC3 cells were transfected with 50 nM control or S100P-targeting siRNA using 10 μl INTERFERin (Autogen Bioclear) for 72 h.

Western blot analysis

Protein lysates were prepared from V3, S5 and BxPC3 cells after knocking down of S100P in NP40 lysis buffer (1 % NP40, 50 mM Tris pH 7.4, 150 mM NaCl with 2× Complete Protease Inhibitor Cocktail tablets, Roche Diagnostics) and quantified using Bradford Assay (Biorad Reagent) with bovine serum albumin as control. 20 μg of protein diluted in SDS–PAGE sample buffer was separated on a NuPAGE 4–12 % Bis–Tris gel (Invitrogen Life Technologies) and transferred onto PVDF Immobilon-P membrane (Millipore, Watford, UK). After blocking with 5 % milk in TBS/1 % Tween 20 the membranes were probed with goat anti-S100P (1:500; R&D Systems, Abingdon, UK) and goat anti-actin (1:2,000; Santa Cruz Biotechnology). The secondary antibody was horseradish peroxidase HRP-conjugated donkey anti-goat Ig (Santa Cruz Biotechnology) diluted 1:2,000 in 5 % milk in TBS/1 % Tween 20. Bound immunocomplexes were detected using enhanced chemiluminescence Western blotting detection reagents (GE Healthcare, Buckinghamshire, UK).

Immunohistochemistry

Immunohistochemical staining was performed on 4 μm paraffin-embedded tissue sections using the Ventana Discovery™ System, Illkirch, France (www.ventanadiscovery.com) following the manufacturer's recommendations. Antibodies used were mouse anti-S100P (dilution 1:25; BD Biosciences), anti-VCAN (1:100, Sigma) and anti-SFN (1:50, Abcam). IHC results were evaluated for both intensity and extent of staining as described previously [14].

For visualisation of collagens, tissue sections were, after de-waxing and hydration, incubated with Sirius Red (VWR, Leicestershire LE17 4XN, UK) for 1 h at room temperature and washed in 1 % acetic acid. Sections were then dehydrated with 100 % ethanol and mounted with DPX Mountant (VWR). In Supplementary Fig. 2, counterstaining to highlight the nuclei was done using Weigert's haematoxylin for 15 min at room temperature.

Transendothelial migration assay

Transendothelial migration assays (TEM) were performed using 6.5 mm transwell inserts with 8 μm pores (BD Biosciences) previously coated with gelatin (50 μl, Sigma) for an hour. 5×10^4 HUVEC cells were seeded (in 200 μl/insert), stimulated with 100 ng/ml IFN-γ for 72 h and incubated at 37 °C and 5 % CO_2 for 24 h. After 24 h medium and non-adherent cells were removed and transendothelial resistance was measured using a MILLICELL-ERS voltmeter (Millipore, USA). The resistance of the endothelial monolayers was determined to be 72 Ω cm^2.

500 µl DMEM medium supplemented with 10 % FCS was then added to the lower compartment, while 5×10^5 S100P-overexpressing (S5) and vector control (V3) cells or 2.5×10^5 BxPC3 cells (all in 200 µl of serum-free medium) were added to the upper compartment on top of the endothelial monolayer. After incubation for 48 h at 37 °C the cells that migrated into the lower compartment were trypsinized and counted using a haemocytometer. All assays were performed in triplicate and on three different days.

Zebrafish embryo xenograft model

Zebrafish (*Danio rerio*) embryos were handled in compliance with local animal care regulations and standard protocols and were kept in an incubator at constant temperature. At 48 h post fertilisation, wild-type and transgenic fli1:enhanced green fluorescent protein (EGFP) zebrafish embryos were dechorionated and anesthetised with 0.003 % Tricaine (Sigma). BxPC3 cells were treated with either control or S100P siRNA and were labelled with fluorescent dyes CMFDA (green) or CMTNR (red), respectively at a 1:1,000 dilution for 15 min according to the manufacturer's protocol (Invitrogen Life Technologies). Equal number of green and red fluorescently labelled cells were mixed prior to injection and re-suspended in Hanks' balanced salt solution (HBSS) at a concentration of 10×10^6/200 µl. Approximately 50–200 BxPC3 cells were injected into the yolk sack of zebrafish embryos using a pressure microinjector (Picospritzer III, Parker, USA). After injection the zebrafish embryos were transferred to water containing 0.03 g/l 1-Phenyl-2-thiourea (PTU) to prevent pigment formation and were kept overnight at 35 °C. At 24 h post-injection embryos were monitored for disseminated cancer cells and the number of invading/migrating cells was counted. Magnification using a 5× objective was used to image the whole body to visualize the spread of the cancer cells throughout the fish embryo and 20× and 40× objectives were used for the localization of cancer cells. A 488 nm laser was used to scan the zebrafish embryo vasculature and a 543 nm laser to scan CMTNR (red)-labelled cancer cells. Embryos were photographed by fluorescent microscopy using Axiovision Rel 4.0 software.

Statistics

All statistical analyses were carried out using the PRISM statistical software package, version 4 (GraphPad, San Diego, CA). All assays were performed at least in triplicate and the statistical analysis performed using the Student's *t* test. For comparison between more than two groups a one-way ANOVA was used. *P* values of <0.05 (*), <0.01 (**) and <0.001 (***) were considered to be statistically significant.

Results

Gene expression profiling

Gene expression profiling was performed on PDAC and unmatched liver metastatic samples and compared to both normal pancreas and normal liver tissues. Unsupervised hierarchical clustering of the most variable 12,000 probes separated all 15 analysed samples into their respective groups (Supplementary Fig. 1). In order to obtain the genes deregulated in common between PDAC and liver metastases two-way ANOVA analysis was performed, which resulted in a subset of 37 probes (corresponding to 33 known genes) that are listed in Table 1, while the heat map constructed based on expression of these genes is shown in Fig. 1. It is evident that most of the genes were commonly up- or down-regulated in both primary PDAC and liver metastases, with number of gene products being an ECM proteins: collagens (COL1A1, COL1A2, COL3A1, COL5A1), VCAN and SERPINF1. Several transcription factors also showed altered expression (EGR1, RUNX1, CNOT2 and FER1L3), as well as adhesion molecules (CTNNB1, ITGAV and ITGB6). In addition, signalling molecules, including SFN and GPRC5A, and well known genes deregulated in PDAC (S100A6, S100P, AGR2) were also seen.

Validation of SFN, VCAN, collagens and S100P

Validation of SFN, VCAN and S100P expression was performed by immunohistochemistry (IHC), while for collagens Sirius red staining was used; all staining was done on ten primary PDACs and their matched metastases (nine from liver and one from lung metastases). Validation of AGR2 expression in metastatic lesions was reported separately [15].

SFN (stratifin, 14-3-3-σ) expression was previously found to increase during PanIN progression [16], and in invasive PDACs [17]; we have recently shown statistically significant increase in SFN protein expression in PDAC metastatic to lymph nodes [18]. Our gene profiling results indicated that this might be the case in liver metastases also (as further suggested by QRT–PCR data of Guweidhi et al. [19]). However, SFN immunoreactivity was found to be largely similar in both primary and metastatic lesions (Fig. 2a, I and II), and increased expression was observed in only one of the liver metastases when compared to the primary tumour (Fig. 2a, III and IV). As the present validation was performed on a limited number of available cases, further validation on a larger series is warranted. Of note, no expression of SFN was noticed in the adjacent histologically normal appearing pancreas and liver (data

Table 1 The 37 common probes in the metastasis-associated gene set

Probe id	Symbol	Name	Tumour effect in pancreas (log_2 fold change)	Tumour effect in liver (log_2 fold change)
202404_s_at	COL1A2	Collagen, type I, alpha 2	5.37	3.97
202310_s_at	COL1A1	Collagen, type I, alpha 1	4.97	3.58
221731_x_at	VCAN	Chondroitin sulfate proteoglycan 2/versican	4.94	2.91
204351_at	S100P	S100 calcium binding protein *P*	4.47	3.89
211161_s_at	COL3A1	Collagen, type III, alpha 1	4.42	2.73
201650_at	KRT19	Keratin 19	4.28	5.92
212488_at	COL5A1	Collagen, type V, alpha 1	4.2	2.28
209173_at	AGR2	Anterior gradient 2 homolog	4.13	4.3
202403_s_at	COL1A2	Collagen, type I, alpha 2	3.89	2.93
230494_at	SLC20A1	Solute carrier family 20 (phosphate transporter), member 1	3.88	3.03
203108_at	GPRC5A	G protein-coupled receptor, family C, group 5, member A	3.35	4.1
33322_i_at	SFN	Stratifin/14-3-3-σ	3.32	4.06
226535_at	ITGB6	Integrin, beta 6	3.3	3.99
204083_s_at	TPM2	Tropomyosin 2 (beta)	3.25	2.53
223631_s_at	C19orf33	Chromosome 19 open reading frame 33	3.05	4.56
33323_r_at	SFN	Stratifin/14-3-3-σ	2.92	4.05
217728_at	S100A6	S100 calcium binding protein A6 (calcyclin)	2.88	3.82
201798_s_at	FER1L3	Fer-1-like 3, myoferlin (*Caenorhabditis elegans*)	2.67	2.93
222449_at	TMEPAI	Transmembrane, prostate androgen induced RNA	2.66	3.54
224559_at	MALAT1	Metastasis-associated lung adenocarcinoma transcript 1 (non-coding RNA)	2.33	2.03
224917_at	TMEM49	Transmembrane protein 49	2.23	2.05
236114_at	RUNX1	Runt-related transcription factor 1 (acute myeloid leukemia 1; aml1 oncogene)	2.14	1.76
236251_at	ITGAV	Integrin, alpha V (vitronectin receptor, alpha polypeptide, antigen CD51)	2.01	2.17
242558_at	CTNNB1	Catenin (cadherin-associated protein), beta 1	1.91	2.73
217733_s_at	TMSB10	Thymosin, beta 10	1.88	2.61
243931_at	CD58	CD58 antigen, (lymphocyte function-associated antigen 3)	1.65	1.64
244197_x_at	CNOT2	CCR4-NOT transcription complex, subunit 2	1.53	2.42
210328_at	GNMT	Glycine N-methyltransferase	−2.18	−3.19
220892_s_at	PSAT1	Phosphoserine aminotransferase 1	−2.77	−1.91
217546_at	MT1 M	Metallothionein 1 M	−2.86	−3.09
205969_at	AADAC	Arylacetamide deacetylase (esterase)	−2.88	−2.57
225207_at	PDK4	Pyruvate dehydrogenase kinase, isozyme 4	−3.05	−2.71
223062_s_at	PSAT1	Phosphoserine aminotransferase 1	−3.93	−3.29
227099_s_at	LOC387763	NA	3.87	−1.78
227404_s_at	EGR1	Early growth response 1	2.98	−2.19
202238_s_at	NNMT	Nicotinamide N-methyltransferase	2.96	−2.83
202283_at	SERPINF1	Serpin peptidase inhibitor, clade F, member 1	2.4	−2.56

not shown); lack of SFN immunoreactivity in normal pancreas and liver was also reported previously [20].

VCAN (versican) was identified as up-regulated in PDAC in our previous gene expression analysis, where it was seen in both the stromal component and in cancer cells [21]. In the present study VCAN expression was evident in the stroma of all nine liver metastases; however it was focal and predominantly surrounding cancerous glands, with

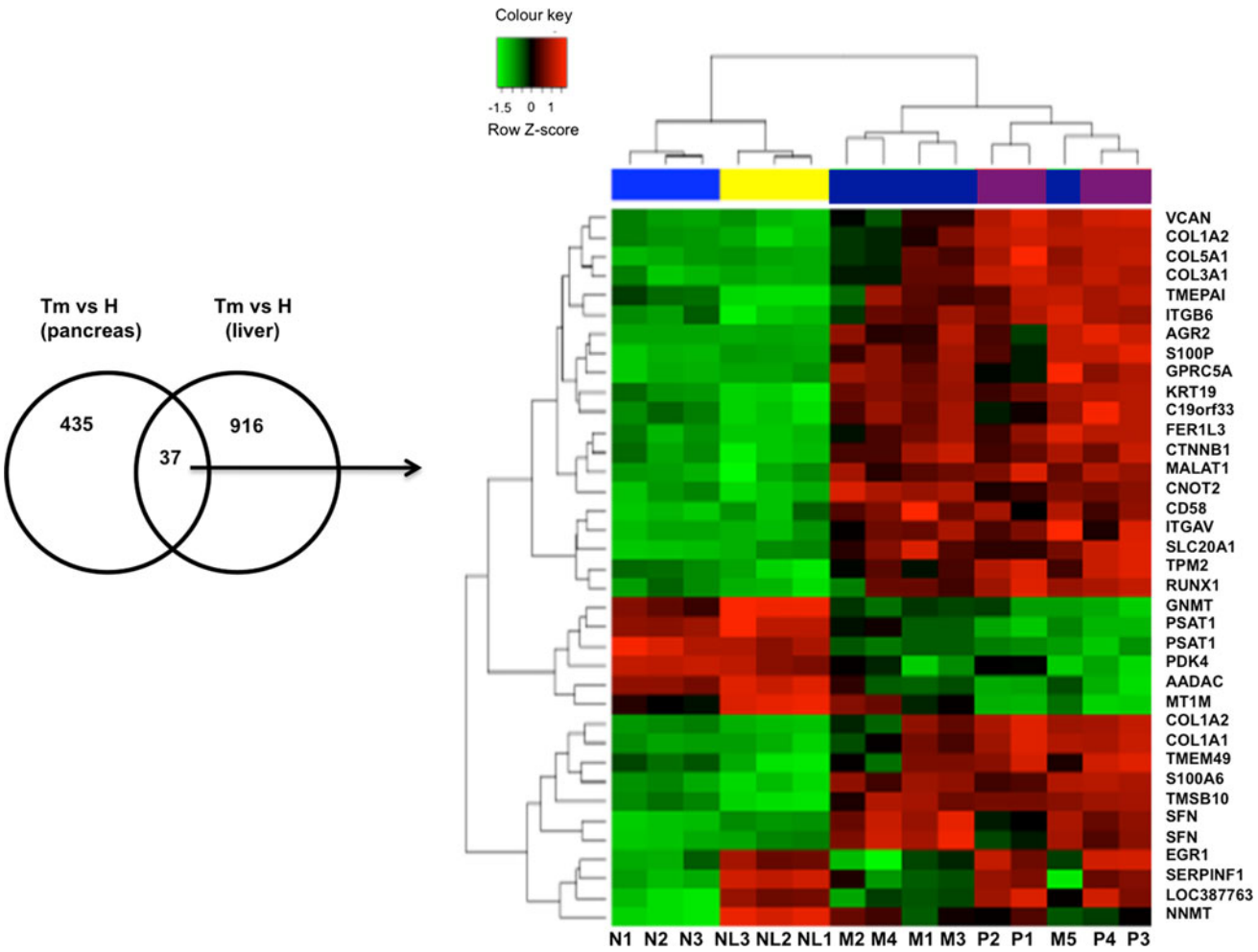

Fig. 1 Metastasis-associated gene set representing 33 genes commonly differentially expressed in primary PDAC and liver metastasis. The Venn diagram on the *left* shows genes differentially expressed in PDAC and metastases versus normal pancreas, 'Tm vs H (pancreas)'; genes differentially expressed in PDAC and liver metastases versus normal liver, 'Tm vs H (liver)', as well as the intersection with 37 gene probes (corresponding to 33 genes) that are present in both primary PDACs and liver metastases. A hierarchical clustering of these 33 unique genes is shown on the *right* hand side. The level of expression for each gene is represented by the intensity of *red* and *green* colour as up- and down-regulated, respectively. N (Normal pancreas, *blue*), NL (Normal liver, *yellow*), M (liver metastasis, *dark blue*) and *P* (Primary PDAC, *violet*). Of note, NL2–NL3 represent technical replicates of the single normal liver specimen. (Color figure online)

intensity varying from weak (Fig. 2b, I) to strong (Fig. 2b, III). Of nine scorable cases, two primary PDACs showed more extensive immunoreactivity, in one case both primary and metastatic tumour showed similar expression, while in five liver metastases VCAN expression was lower than in matched primary PDAC (Fig. 2b, IV); lung metastases had no stromal component, hence no VCAN was seen (Fig. 2b, II). While weak or no VCAN was seen in histologically normal appearing pancreas, in six out of nine cases VCAN immunoreactivity was observed in the cytoplasm of hepatocytes adjacent to cancer (as seen in Fig. 2b, IV); this could be due to induction of VCAN expression, as no staining was seen in the normal liver (data not shown).

The amount of stromal collagen was assessed after Sirius Red staining and while zonal heterogeneity was seen, in approximately half of liver metastases, lower levels of collagen were noticed (Fig. 2c, III compared to IV; malignant ducts and hepatocytes are stained yellow while collagen fibres are red; 2c, I and II are the same tissue samples stained with Haematoxylin and Eosin and are included for easier histological interpretation). Furthermore, collagen fibres appeared less organised (Supplementary Fig. 2).

The involvement of S100P in tumour growth, migration and invasion of PDAC cells was previously reported by our group and others [9, 10], and it was therefore selected for further validation and functional analysis. High levels of S100P expression in primary PDAC and liver metastases were seen both by QRT–PCR and IHC (Fig. 3a, b, respectively). QRT–PCR data validated the increased

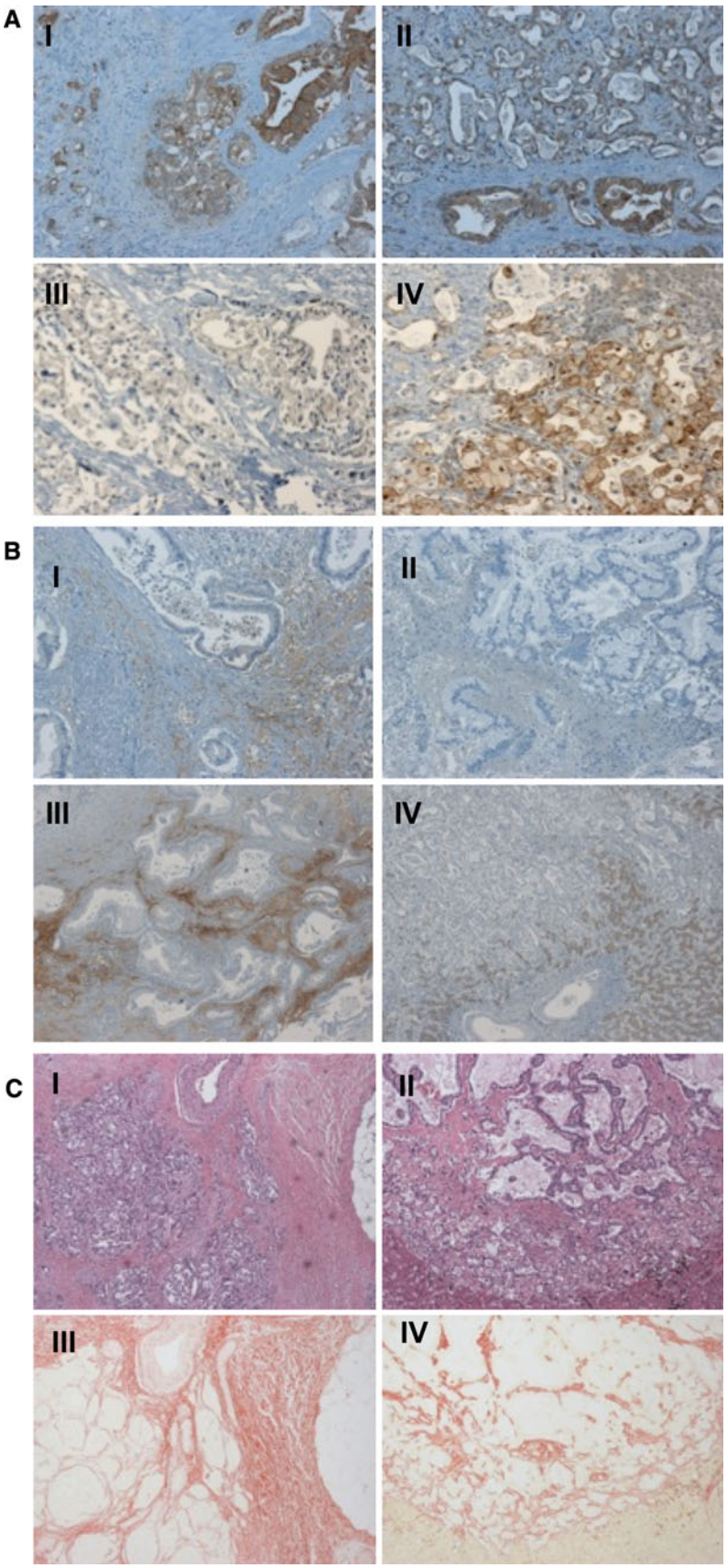

Fig. 2 Validation of gene profiling data. **a** Representative images of SFN expression; similar immunoreactivity in the primary and in the matched liver metastasis was seen in *I* and *II*, respectively; while weaker expression in the primary tumour (*III*) and stronger in matched liver metastases (*IV*) was seen in the second case; all images ×100. **b** VCAN immunoreactivity in the stroma surrounding malignant glands in the primary PDAC is seen on (*I*, *III*), while lack of expression of VCAN was noticed in their matched lung (*II*) and liver (*IV*) metastases. Of note, some staining in adjacent hepatocytes was also seen. Two primary PDAC cases (*I* and *III*) demonstrate variable expression; *I* and *II* magnification ×100; *III* and *IV* ×50. **c** Sirius Red staining for collagen. Primary PDAC shown in *III* displays abundant collagen, which appears less abundant in stroma of liver metastatic lesion (*IV*). Haematoxylin and Eosin-stained sections of the same cases (primary PDAC in *I* and liver metastases in *II*) are provided for easier orientation (all magnified ×50)

expression of S100P in all the tumour samples used for Affymetrix analysis as well as in two additional primary PDACs (PDAC5 and PDAC6). High S100P expression was seen in the cytoplasm and nucleus of all primary PDAC (Fig. 3b, I, III and V) and matched liver (Fig. 3b, II and IV) and lung (Fig. 3b, VI) metastases, and in general, the intensity and extent of staining was similar in the two types of lesions. Of note, a lack of S100P immunoreactivity in normal pancreas and liver has been previously established [22, 23].

Role of S100P in the TEM

To systematically investigate the functional significance of this molecule in the metastatic process, we decided to study the next key step in the metastatic process i.e. TEM of cancer cells. A schematic representation of the assay used is shown in Fig. 4a. It was performed with previously engineered Panc1 cells that stably over-express S100P (S5 cells) or vector control (V3) cells [10], as well as after S100P-targeted siRNA treatment. The silencing of S100P in S5 cells was confirmed by QRT–PCR and Western blot (Fig. 4b, I and II, respectively). The results showed increased TEM of S5 cells when compared to control V3 cells; in contrast, knockdown of S100P in S5 cells significantly decreased the number of transmigrating cells (Fig. 4b, III). This finding was validated using an additional pancreatic cancer cell line, BxPC3, which expresses high levels of endogenous S100P [9]. After successful S100P silencing (Fig. 4c, I and II) a statistically significant decrease in cancer cell migration through the endothelial monolayer is seen (Fig. 4c, III).

To validate these in vitro findings, we investigated the role of S100P in the dissemination of PDAC cells in vivo using a zebrafish embryo model as described previously [15]. BxPC3 cells treated with control siRNA were labelled with CMFDA (green) and S100P siRNA treated cells with CMTNR (red) fluorescent dye; subsequently, labelled cells were mixed and injected into the yolk sack of 48 h post-fertilization zebrafish embryos. Cancer cell dissemination was observed in living fish embryos by fluorescent microscopy 24 h post-injection (Fig. 5a). Control siRNA treated BxPC3 cells were observed in the head, eye, trunk, tail as well as in the vasculature, whereas S100P-silenced BxPC3 cells mostly remained in the yolk sack. Of note, swapping of the dyes had no influence on the results, and no differences in the proliferation or survival of control or S100P siRNA treated BxPC3 cells were noticed within the duration of the experiments (data not shown).

In order to clearly visualize cancer cells in the blood vessels we used transgenic zebrafish fli1:EGFP, which possess green fluorescent vasculature. Since in wild-type embryos it is very difficult to judge whether migrating/invading cells are inside or outside the blood vessels due to their transparency, fli1:EGFP embryos are a perfect model for the analysis of tumour cell-blood vessel interaction. BxPC3 cells labelled with CMTNR (red) fluorescent dye were injected in these fli1:EGFP embryos and analysed 24 h post-injection. The top panel (I) of Fig. 5b shows a

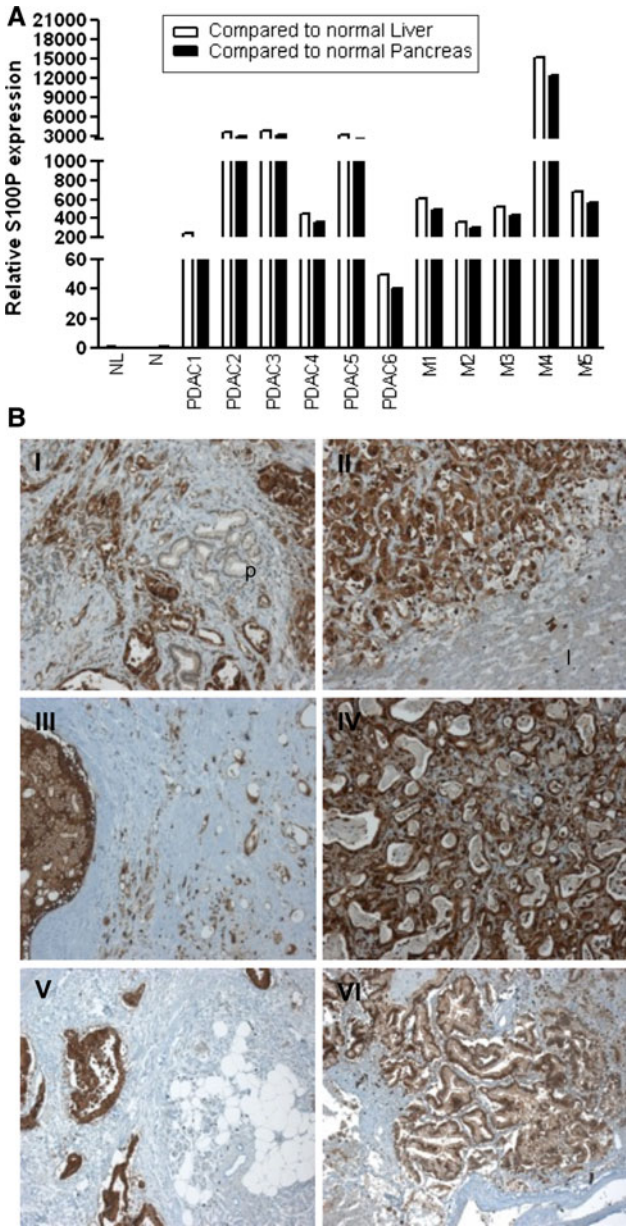

Fig. 3 Confirmation of high expression of S100P in both PDACs and liver metastases using QRT–PCR and IHC. **a** QRT–PCR analysis shows high levels (>40 fold) of S100P expression in primary PDACs (PDAC1–PDAC6) and liver metastatic specimens (M1–M5) compared to normal tissues (pancreas and liver). **b** Immunohistochemical analysis: representative images show strong cytoplasmic and nuclear S100P immunoreactivity in primary (*I*, *III*, *V*) and their matched liver (*II*, *IV*) and lung (*VI*) metastases. Note much weaker expression in PanIN lesions ('p') on *I*. 'l' on image *II* indicates adjacent histologically normal liver. *I*, *II*, *V* and *VI* magnification ×50; *III* and *IV* magnification ×100

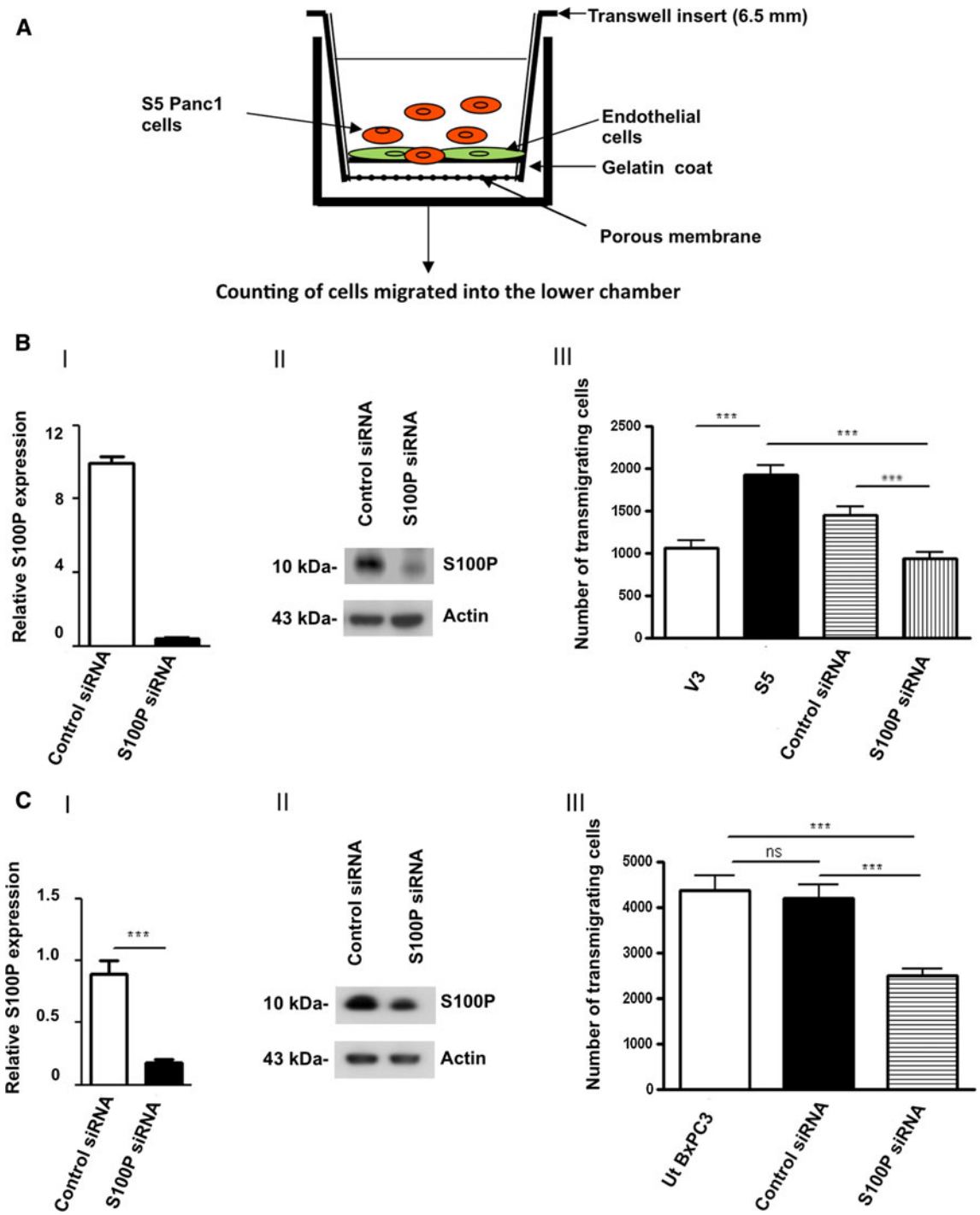

Fig. 4 Trans-endothelial migration assays following over-expression and knock-down of S100P in Panc1 and BxPC3 cells. **a** Schematic representation of TEM. **b** Knock-down of S100P in S100P-over-expressing Panc1 cells was confirmed by QRT–PCR (*I*) and Western blot, with actin as a loading control (*II*). Trans-endothelial migration assays of S100P-over-expressing Panc1 cells (S5), the vector control (V3) cells and S5 cells following treatment with either S100P or control siRNA are shown on III. A statistically significant increase in the number of trans-migrating S5 cells in comparison to V3 cells was seen ($P < 0.001$); inversely, a significant decrease in the number of intravasating cells after S100P silencing when compared to both untreated and control siRNA treated S5 cells was observed (both $P < 0.001$). A mean number of transmigrating cells and the standard error of the mean from three independent experiments are shown. **c** Knock-down of S100P in BxPC3 cells was confirmed by QRT–PCR (*I*) and Western blot with actin as a loading control (*II*). Trans-endothelial migration assays of untreated BxPC3 cells (Ut BxPC3) and BxPC3 cells after the treatment with either control or S100P siRNA are shown on *III*. Both untreated and control siRNA-transfected BxPC3 cells showed statistically significant higher levels of in trans-endothelial migration compared to BxPC3 cells after S100P silencing ($P < 0.001$). *Bar* charts show the mean number of transmigrating cells with the SE of the mean from three independent experiments

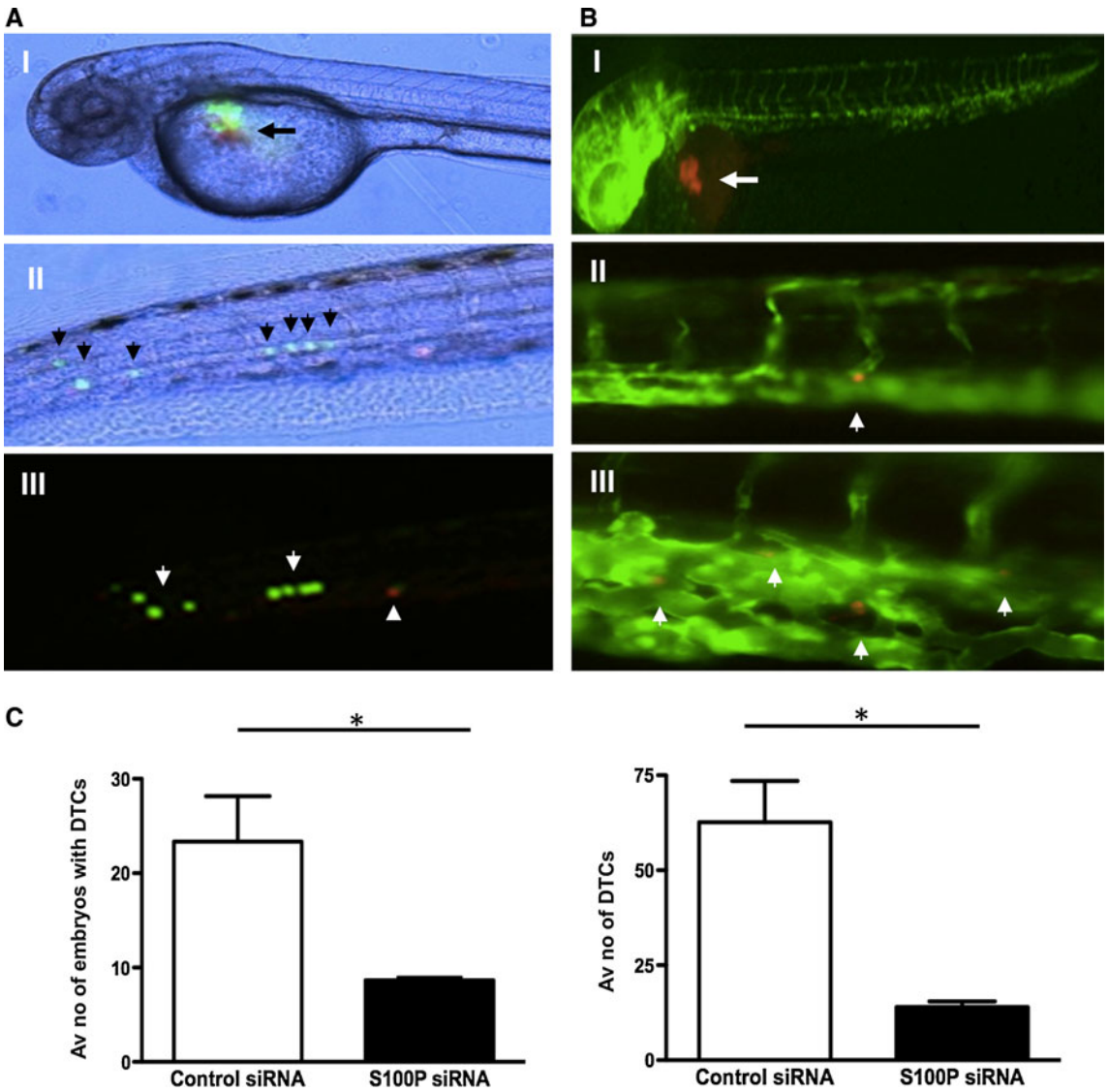

Fig. 5 Knock-down of S100P decreases metastatic potential of BxPC3 cells in zebrafish embryos. **a** An equal number of BxPC3 cells transfected either with control siRNA (labelled with CMFDA *green dye*) or S100P siRNA (labelled with CMTNR *red dye*) were co-injected into the yolk sack of 48 h post-fertilization (hpf) wild-type zebrafish embryos. Cancer cell dissemination was evaluated at 24 h post-injection by brightfield (*II*) and fluorescent (*III*) microscopy. A representative image of a 48 hpf wild-type zebrafish embryo injected with labelled 50–200 BxPC3 cells is shown on *I* (*arrow* indicates the injection site). A representative wild-type zebrafish embryo at 24 h post-injection shows that BxPC3 cells treated with control siRNA invaded/migrated more readily from the yolk to the distant sites of the embryo (indicated by *arrows*) (*II*). Fluorescent image of the same embryo shows several fluorescently labelled green BxPC3 cells and one *red* control cell (*arrowhead*) in the same area of the zebrafish embryo (*III*). **b** Metastasis of BxPC3 cells visualized in transgenic fli1:EGFP zebrafish embryos. The fluorescent image of Transgenic fli1:EGFP zebrafish embryo injected with BxPC3 cells labelled with CMTNR (*red*) dye into the yolk sack of 48 h post-fertilization (*arrow* indicated the injection site) (*I*). Single BxPC3 cell (in *red*) entering/exiting the inter-segmental vessel of a Tg (fli1:EGFP) zebrafish embryo (*II*). Cancer cells (indicated by *arrows*) are embedded in the caudal vein plexus, some are inside the blood vessels and some are coming out from the vessels of fli1:EGFP zebrafish embryo (*III*). Images were taken by fluorescent microscopy at injection and 24 h post-injection, original magnification ×100 (*I*) and ×400 (*II* and *III*). In **a/b** *II* and *III*: anterior is to *right*, dorsal to *top*. **c** *Left panel*, *bar* charts show the average number of zebrafish embryos with disseminated tumour cells (DTC) from three independent experiments and demonstrate the decreased metastatic potential of BxPC3 cells treated with S100P siRNA compared to non-targeting control siRNA ($P = 0.047$). *Right panel*, quantification of numbers of migrated cells at 24 h post-injection in total of 70 embryos is shown. Numbers of DTC from three independent experiments are shown. Silencing of S100P in BxPC3 cells led to decreased number of DTCs compared to non-targeting control siRNA ($P = 0.019$). (Color figure online)

representative image of a 48 h-old fli1:EGFP embryo with fluorescently labelled cancer cells in the yolk sack (arrow); this image was taken immediately after injection. Panels (II) and (III) show the BxPC3 cells in the vasculature. Some cells were visible inside the blood vessels, caudal vein plexus and inter segmental vessels. Quantification of

the microinjection results demonstrated that of a total of 115 injected embryos across the three experiments, 70 (33 + 19 + 18, average 23.3) embryos injected with control siRNA treated BxPC3 cells showed dissemination of cancer cells (61 %), in contrast to only 26 (9 + 8 + 9, average 8.6) embryos (23 %) injected with BxPC3 in which S100P was silenced (Fig. 5c, left panel). Hence, there were almost three times more embryos with disseminated cancer cells after S100P silencing ($P = 0.04$). The average number of migrating BxPC3 cells treated with control siRNA was 63 (73, 74 and 41 in each experiment, respectively) as compared to 14 (13, 17 and 12 in each experiment, respectively) S100P-siRNA treated cells, $P = 0.019$ (Fig. 5c, right panel).

These findings provide evidence that S100P plays an important role in the intravasation of PDAC cells and hence facilitates the early steps in the metastatic process leading to haematogenous spread and liver metastases.

Discussion

A large body of evidence suggests that gene profiles of metastatic lesions in many different cancer types are highly similar to their cancers of origin [5–8]. Our study was therefore designed to explore a common set of the most differentially expressed genes in both PDAC and liver metastases when compared to normal pancreatic and liver tissues. We obtained a set of 33 metastasis-associated genes, which represent a pool of critically needed, potential metastatic disease-based therapeutic targets.

Interestingly, comparison of these 33 genes with data from profiling studies of PDAC precursor lesions, PanINs ([24, 25] and our unpublished data) revealed that almost one-third of these genes, including 14-3-3-σ, EGR1, AGR2, S100A6, S100P, GPRC5A, COL1A1, PSAT1 and AADAC were already deregulated in these early lesions. This finding not only supports the recent evidence that the metastatic potential of human cancers is present in the bulk of a primary tumour [26–28] but, additionally, that genes conferring metastatic potential in PDAC seem to be encoded early in pancreatic tumour development. With the exception of PSAT1 and AADAC, enzymes whose diminished expression probably reflect loss of acinar cells, all other genes, including AGR2 and S100A6 have already been shown to increase invasiveness of PDAC cancer cells [15, 29–31]. Of 33 metastasis-associated genes, more than 20 % were shown to code for ECM proteins, VCAN and collagens were therefore selected for validation at the protein level.

VCAN is a member of the family of large aggregating chondroitin sulphate proteoglycans. It has been reported in a variety of tumours and its over-expression has been correlated with poor prognosis in several cancers (for review see [32]). In pancreatic cancer it has been demonstrated that VCAN can be secreted by pancreatic cancer cells [33], and that elevated levels of post-translationally modified VCAN are associated with the malignant phenotype of PDAC playing a crucial role in tumour progression [34]. Sakko et al. [35] recently reported that increased expression of VCAN could facilitate tumour invasion and metastasis in prostate cancer by decreasing the cancer cell-ECM adhesion; whether this is also the case in the pancreatic cancer still remains to be established.

Collagens, in particular COL1A1 and COL3A1, are principal constituents of pancreatic desmoplastic stroma [36]. It was recently shown that type I collagens stimulate migration and metastatic behaviour of PDAC cells through Src-dependent down-regulation of E-cadherin [37]; collagen I also activates JNK, which up-regulates N-cadherin, initiates EMT and promotes invasion and metastasis [38]. In addition, pancreatic stellate cells, major producers of collagenous matrices, not only promote PDAC progression [39], but can also accompany cancer cells to metastatic sites in an orthotopic mouse model [40]. The general importance of collagenous stroma was highlighted in several studies where COL1A1 and COL1A2 were shown to be components of global metastatic gene signatures (for review see [41]). Interestingly, it was also shown that spatial reorganisation of collagen matrices can be used for the prediction and monitoring of the invasiveness of cancer cells using multiphoton laser-scanning microscopy in living (breast cancer) tissues [42]. Based on our profiling data, lower levels of expression of collagen genes were seen in liver metastases, which were also noted at the protein level in half of cases used for validation. This would corroborate a recent report that the lower deposition of collagen correlates with shorter survival and is an independent predictor of poor prognosis in pancreatic cancer patients [43]. Furthermore, no collagenous stroma was observed in a case of the lung metastatic lesion examined; a complete absence of stroma in 20 % of PDAC lung metastases was previously reported [11]. In our recent analysis of primary PDAC and lymph node metastases [18], out of 16 pairs, three had similar amount of stroma in both primary tumour and metastases, one case showed more abundant stroma in lymph node metastasis while in 12 cases (75 %) less stroma was seen in metastatic lymph nodes than in the primary PDAC. Further evaluation of both the quantity and 'quality' of stroma in metastatic lesions and the interaction of stromal proteins with cancer cells that have now reached their full metastatic competency is therefore warranted.

Compelling evidence that S100P plays a significant role in tumour progression and metastasis of different cancer types, including PDAC is already available. In breast cancer, subcutaneous injection of (otherwise nonmetastatic) rat mammary cells transfected with S100P cDNA

induced metastases in syngeneic rats [44]; in non-small cell lung cancer (NSCLC), S100P over-expression was found to be a strong predictor of distant metastasis [45]. A recent study using a mouse xenograft model has shown that S100P overexpression correlated with increased angiogenesis and metastasis, while silencing of endogenous S100P decreased angiogenesis, tumour growth and metastasis in lung cancer [46]. Similarly, in the pancreatic orthotopic mouse model, knockdown of S100P expression significantly reduced tumour growth and metastasis in lung and liver [9]; here, we demonstrate that S100P is highly expressed in human primary PDAC and all the liver and the one lung metastasis tested. The detailed roles of S100P in the metastatic process are, however, still largely unknown.

We have previously shown that over-expression of S100P in Panc1 pancreatic cancer cells increases expression of cathepsin D, which facilitates local invasion by ECM remodeling [10] thus increasing their invasive potential; now we demonstrate that, in addition to local invasion, S100P is also involved in trans-endothelial migration which is a crucial step for initiation of distant metastasis. This was also recently seen in lung cancer [45]. While underlying mechanisms in PDAC still remain to be explored, in NSCLC Ca^{2+}-dependent ezrin–S100P interaction was shown to play an important role in promoting such TEM [47, 48].

In order to recapitulate the in vitro TEM assay in vivo, we have used the zebrafish embryo as a model. Zebrafish have been used to study cancer progression and metastatic behaviour of cancer cells extensively [49–51]. There are many advantages to this model including that it is inexpensive, and that immunoprivileged and transparent embryos can be used to study cancer cell invasion and migration directly. Our data demonstrated that knockdown of S100P can significantly reduce the metastatic behavior of BxPC3 cells, which is fully consistent with our in vitro data. We have found that at 24 h post-injection BxPC3 cells migrated from the injection site (yolk sack), entered into the vasculature and travelled to the distant parts of the embryo compared to the BxPC3 cells with silenced S100P. While a short duration of the assay precluded the studying of the fate of cancer cells at the later time points, disseminated BxPC3 cells in the vasculature visualized in fli1: EGFP embryos, suggested that S100P plays a critical role in haematogenous spread of pancreatic cancer cells, which firmly establishes its role in the initiation and progression steps [52] of the metastatic cascade.

In summary, we describe a set of 33 metastasis-associated genes in PDAC and related liver metastases. Although not all of these genes might be directly involved in the metastatic process per se they could serve as biomarkers of malignant disease. However, functionally involved genes such as S100P could well represent an invaluable resource of potential novel therapeutic targets, and these are critically needed to improve the currently bleak prognosis of PDAC patients.

Acknowledgments We thank G. Elia for help with collagen staining and Prof. I. Hart for critical reading of the manuscript. This work is funded by the Barts and the London Charitable Foundation (SB), Cancer Research UK C355/A6253 (CC, TCJ, NRL) and HEFCE (TCJ). We are grateful to Dr. Iacobuzio-Donahue for kindly providing us with pancreatic cancer primary and liver metastatic samples from the GICRMDP at John Hopkins University, Baltimore, USA.

Conflicts of interest The authors declare that they have no conflict of interest.

References

1. Jemal A, Siegel R, Ward E, Hao Y, Xu J, Murray T et al (2008) Cancer statistics. CA Cancer J Clin 58(2):71–96
2. Kamisawa T, Isawa T, Koike M, Tsuruta K, Okamoto A (1995) Hematogenous metastases of pancreatic ductal carcinoma. Pancreas 11(4):345–349
3. Yachida S, Jones S, Bozic I, Antal T, Leary R, Fu B et al (2010) Distant metastasis occurs late during the genetic evolution of pancreatic cancer. Nature 467(7319):1114–1117
4. Niedergethmann M, Alves F, Neff JK, Heidrich B, Aramin N, Li L et al (2007) Gene expression profiling of liver metastases and tumour invasion in pancreatic cancer using an orthotopic SCID mouse model. Br J Cancer 97(10):1432–1440
5. Campagna D, Cope L, Lakkur SS, Henderson C, Laheru D, Iacobuzio-Donahue CA (2008) Gene expression profiles associated with advanced pancreatic cancer. Int J Clin Exp Pathol 1(1):32–43
6. Inamura K, Shimoji T, Ninomiya H, Hiramatsu M, Okui M, Satoh Y et al (2007) A metastatic signature in entire lung adenocarcinomas irrespective of morphological heterogeneity. Hum Pathol 38(5):702–709
7. Ellsworth RE, Seebach J, Field LA, Heckman C, Kane J, Hooke JA et al (2009) A gene expression signature that defines breast cancer metastases. Clin Exp Metastasis 26(3):205–213
8. D'Arrigo A, Belluco C, Ambrosi A, Digito M, Esposito G, Bertola A et al (2005) Metastatic transcriptional pattern revealed by gene expression profiling in primary colorectal carcinoma. Int J Cancer 115(2):256–262
9. Arumugam T, Simeone DM, Van Golen K, Logsdon CD (2005) S100P promotes pancreatic cancer growth, survival, and invasion. Clin Cancer Res 11(15):5356–5364
10. Whiteman HJ, Weeks ME, Dowen SE, Barry S, Timms JF, Lemoine NR et al (2007) The role of S100P in the invasion of pancreatic cancer cells is mediated through cytoskeletal changes and regulation of cathepsin D. Cancer Res 67(18):8633–8642
11. Embuscado EE, Laheru D, Ricci F, Yun KJ, de Boom Witzel S, Seigel A et al (2005) Immortalizing the complexity of cancer metastasis: genetic features of lethal metastatic pancreatic cancer obtained from rapid autopsy. Cancer Biol Ther 4(5):548–554
12. Smyth GK (2004) Linear models and empirical bayes methods for assessing differential expression in microarray experiments. Stat Appl Genet Mol Biol 3:Article3
13. Smyth GK, Michaud J, Scott HS (2005) Use of within-array replicate spots for assessing differential expression in microarray experiments. Bioinformatics 21(9):2067–2075
14. Neesse A, Gangeswaran R, Luettges J, Feakins R, Weeks ME, Lemoine NR et al (2007) Sperm-associated antigen 1 is expressed early in pancreatic tumorigenesis and promotes motility of cancer cells. Oncogene 26(11):1533–1545

15. Dumartin L, Whiteman HJ, Weeks ME, Hariharan D, Dmitrovic B, Iacobuzio-Donahue CA et al (2011) AGR2 is a novel surface antigen that promotes the dissemination of pancreatic cancer cells through regulation of cathepsins B and D. Cancer Res 71(22): 7091–7102
16. Maitra A, Adsay NV, Argani P, Iacobuzio-Donahue C, De Marzo A, Cameron JL et al (2003) Multicomponent analysis of the pancreatic adenocarcinoma progression model using a pancreatic intraepithelial neoplasia tissue microarray. Mod Pathol 16(9): 902–912
17. Iacobuzio-Donahue CA, Maitra A, Olsen M, Lowe AW, van Heek NT, Rosty C et al (2003) Exploration of global gene expression patterns in pancreatic adenocarcinoma using cDNA microarrays. Am J Pathol 162(4):1151–1162
18. Naidoo K, Jones R, Dmitrovic B, Wijesuriya N, Kocher H, Hart IR et al (2011) Proteome of formalin-fixed paraffin-embedded pancreatic ductal adenocarcinoma and lymph node metastases. J Pathol 226(5):756–763
19. Guweidhi A, Kleeff J, Giese N, El Fitori J, Ketterer K, Giese T et al (2004) Enhanced expression of 14-3-3sigma in pancreatic cancer and its role in cell cycle regulation and apoptosis. Carcinogenesis 25(9):1575–1585
20. Nakajima Shimooka H, Weixa P, Segawa A, Motegi A, Jian Z et al (2003) Immunohistochemical demonstration of 14–3-3 sigma protein in normal human tissues and lung cancers, and the preponderance of its strong expression in epithelial cells of squamous cell lineage. Pathol Int 53(6):353–360
21. Crnogorac-Jurcevic T, Efthimiou E, Capelli P, Blaveri E, Baron A, Terris B et al (2001) Gene expression profiles of pancreatic cancer and stromal desmoplasia. Oncogene 20(50):7437–7446
22. Crnogorac-Jurcevic T, Missiaglia E, Blaveri E, Gangeswaran R, Jones M, Terris B et al (2003) Molecular alterations in pancreatic carcinoma: expression profiling shows that dysregulated expression of S100 genes is highly prevalent. J Pathol 201(1):63–74
23. Parkkila S, Pan PW, Ward A, Gibadulinova A, Oveckova I, Pastorekova S et al (2008) The calcium-binding protein S100P in normal and malignant human tissues. BMC Clin Pathol 8:2
24. Sitek B, Sipos B, Alkatout I, Poschmann G, Stephan C, Schulenborg T et al (2009) Analysis of the pancreatic tumor progression by a quantitative proteomic approach and immunohistochemical validation. J Proteome Res 8(4):1647–1656
25. Buchholz M, Braun M, Heidenblut A, Kestler HA, Kloppel G, Schmiegel W et al (2005) Transcriptome analysis of microdissected pancreatic intraepithelial neoplastic lesions. Oncogene 24(44):6626–6636
26. van 't Veer LJ, Dai H, van de Vijver MJ, He YD, Hart AA, Mao M et al (2002) Gene expression profiling predicts clinical outcome of breast cancer. Nature 415(6871):530–536
27. Weigelt B, Glas AM, Wessels LF, Witteveen AT, Peterse JL, van't Veer LJ (2003) Gene expression profiles of primary breast tumors maintained in distant metastases. Proc Natl Acad Sci USA 100(26):15901–15905
28. Ramaswamy S, Ross KN, Lander ES, Golub TR (2003) A molecular signature of metastasis in primary solid tumors. Nat Genet 33(1):49–54
29. Vimalachandran D, Greenhalf W, Thompson C, Luttges J, Prime W, Campbell F et al (2005) High nuclear S100A6 (Calcyclin) is significantly associated with poor survival in pancreatic cancer patients. Cancer Res 65(8):3218–3225
30. Ohuchida K, Mizumoto K, Ishikawa N, Fujii K, Konomi H, Nagai E et al (2005) The role of S100A6 in pancreatic cancer development and its clinical implication as a diagnostic marker and therapeutic target. Clin Cancer Res 11(21):7785–7793
31. Ramachandran V, Arumugam T, Wang H, Logsdon CD (2008) Anterior gradient 2 is expressed and secreted during the development of pancreatic cancer and promotes cancer cell survival. Cancer Res 68(19):7811–7818
32. Ricciardelli C, Sakko AJ, Ween MP, Russell DL, Horsfall DJ (2009) The biological role and regulation of versican levels in cancer. Cancer Metastasis Rev 28(1–2):233–245
33. Mauri P, Scarpa A, Nascimbeni AC, Benazzi L, Parmagnani E, Mafficini A et al (2005) Identification of proteins released by pancreatic cancer cells by multidimensional protein identification technology: a strategy for identification of novel cancer markers. FASEB J 19(9):1125–1127
34. Skandalis SS, Kletsas D, Kyriakopoulou D, Stavropoulos M, Theocharis DA (2006) The greatly increased amounts of accumulated versican and decorin with specific post-translational modifications may be closely associated with the malignant phenotype of pancreatic cancer. Biochim Biophys Acta 1760(8): 1217–1225
35. Sakko AJ, Ricciardelli C, Mayne K, Suwiwat S, LeBaron RG, Marshall VR et al (2003) Modulation of prostate cancer cell attachment to matrix by versican. Cancer Res 63(16):4786–4791
36. Gress TM, Muller-Pillasch F, Lerch MM, Friess H, Buchler M, Adler G (1995) Expression and in situ localization of genes coding for extracellular matrix proteins and extracellular matrix degrading proteases in pancreatic cancer. Int J Cancer 62(4): 407–413
37. Menke A, Philippi C, Vogelmann R, Seidel B, Lutz MP, Adler G et al (2001) Down-regulation of E-cadherin gene expression by collagen type I and type III in pancreatic cancer cell lines. Cancer Res 61(8):3508–3517
38. Shintani Y, Hollingsworth MA, Wheelock MJ, Johnson KR (2006) Collagen I promotes metastasis in pancreatic cancer by activating c-Jun NH(2)-terminal kinase 1 and up-regulating N-cadherin expression. Cancer Res 66(24):11745–11753
39. Hwang RF, Moore T, Arumugam T, Ramachandran V, Amos KD, Rivera A et al (2008) Cancer-associated stromal fibroblasts promote pancreatic tumor progression. Cancer Res 68(3): 918–926
40. Xu Z, Vonlaufen A, Phillips PA, Fiala-Beer E, Zhang X, Yang L et al (2010) Role of pancreatic stellate cells in pancreatic cancer metastasis. Am J Pathol 177(5):2585–2596
41. Albini A, Mirisola V, Pfeffer U (2008) Metastasis signatures: genes regulating tumor-microenvironment interactions predict metastatic behavior. Cancer Metastasis Rev 27(1):75–83
42. Provenzano PP, Inman DR, Eliceiri KW, Knittel JG, Yan L, Rueden CT et al (2008) Collagen density promotes mammary tumor initiation and progression. BMC Med 6:11
43. Erkan M, Michalski CW, Rieder S, Reiser-Erkan C, Abiatari I, Kolb A et al (2008) The activated stroma index is a novel and independent prognostic marker in pancreatic ductal adenocarcinoma. Clin Gastroenterol Hepatol 6(10):1155–1161
44. Wang G, Platt-Higgins A, Carroll J, de Silva Rudland S, Winstanley J, Barraclough R et al (2006) Induction of metastasis by S100P in a rat mammary model and its association with poor survival of breast cancer patients. Cancer Res 66(2):1199–1207
45. Diederichs S, Bulk E, Steffen B, Ji P, Tickenbrock L, Lang K et al (2004) S100 family members and trypsinogens are predictors of distant metastasis and survival in early-stage non-small cell lung cancer. Cancer Res 64(16):5564–5569
46. Bulk E, Hascher A, Liersch R, Mesters RM, Diederichs S, Sargin B et al (2008) Adjuvant therapy with small hairpin RNA interference prevents non-small cell lung cancer metastasis development in mice. Cancer Res 68(6):1896–1904
47. Austermann J, Nazmi AR, Muller-Tidow C, Gerke V (2008) Characterization of the Ca2+—regulated ezrin–S100P interaction and its role in tumor cell migration. J Biol Chem 283(43): 29331–29340

48. Koltzscher M, Neumann C, Konig S, Gerke V (2003) Ca2+—dependent binding and activation of dormant ezrin by dimeric S100P. Mol Biol Cell 14(6):2372–2384
49. Marques IJ, Weiss FU, Vlecken DH, Nitsche C, Bakkers J, Lagendijk AK et al (2009) Metastatic behaviour of primary human tumours in a zebrafish xenotransplantation model. BMC Cancer 9:128
50. Goessling W, North TE, Zon LI (2007) New waves of discovery: modeling cancer in zebrafish. J Clin Oncol 25(17):2473–2479
51. Stoletov K, Montel V, Lester RD, Gonias SL, Klemke R (2007) High-resolution imaging of the dynamic tumor cell vascular interface in transparent zebrafish. Proc Natl Acad Sci USA 104(44): 17406–17411
52. Nguyen DX, Bos PD, Massague J (2009) Metastasis: from dissemination to organ-specific colonization. Nat Rev Cancer 9(4): 274–284